https://doi.org/10.48048/tis.2025.9396

Efficient Synthesis using One-Pot Method and *In Silico* Analysis of Pyridazinone Derivatives as Inhibitor for Aldose Reductase Enzymes

Yuni Fatisa[1,2], Noval Herfindo[1], Fadila Aisyah[1], Hilwan Yuda Teruna[1], Jasril Jasril[1,*], Adel Zamri[1] and Neni Frimayanti[3]

[1]Department of Chemistry, Faculty of Mathematics and Natural Sciences, Universitas Riau, Pekanbaru 28293, Indonesia
[2]Department of Chemistry Education, Faculty of Tarbiyah and Keguruan, Universitas Islam Negeri Sultan Syarif Kasim, Kampar 28293, Indonesia
[3]Department of Pharmacy, Sekolah Tinggi Ilmu Farmasi Riau, Pekanbaru 28293, Indonesia

([*]Corresponding author's e-mail: jasril.k@lecturer.unri.ac.id)

Received: 26 November 2024, Revised: 26 December 2024, Accepted: 2 January 2025, Published: 28 February 2025

Abstract

This research aims to synthesize a series of pyridazinone derivatives (4a-4d, 5, 6a-6d), investigate their activities against the aldose reductase enzyme, and analyze their pharmacology profiles. Substituted-acetophenone were reacted with glyoxylic acid and hydrazine through a one-pot process using a heating reactor to obtain compounds 4a - 4d. Meanwhile, compounds 5 and 6a - 6d using a stirring technique, were synthesized combining compound 4d with *p*-chloro benzene sulphonic acid for compound 5 and combining compounds 4a - 4d with ethyl chloro acetate to produce compounds 6a - 6d. The MOE 2021.010 software package was taken to perform the molecular docking analysis. The ADMET profiles were performed using online pre-ADME and ProTox II. In this research, 9 pyridazinone derivatives (4a-4d, 5, and 6a-6d) were synthesized. Three of them are new compounds, namely 6a, 6b, and 5. The docking results predicted that compound 5 exhibits the best inhibition against the aldose reductase with a binding free energy value of −12.61 kcal/mol. The tolrestat as positive control has binding free energy values of −14.13 kcal/mol. Compound 5 binds with essential residues at the active site, which builds 5 hydrogen bonds with His110, Tyr48, Cys298, and Asn160 and 3 hydrophobic interactions with His110, Trp111, and Tyr209. The ADMET result provides information about the pharmacotherapy potential of all molecules. But for compound 5, structure modification is needed to improve its safety, especially to remove its hepatoxicity. This information could support that compound **5** can be considered as a reference for further drug design development to be a potential agent for aldose reductase enzymes inhibitor.

Keywords: ADMET, Aldose reductase, *In silico* analysis, Molecular docking, One-pot synthesis, Pyridazinone

Introduction

Diabetes mellitus (DM) is a long-term metabolic disorder caused by impaired insulin production, insulin resistance, or both, leading to hyperglycemia or high blood glucose levels [1,2]. High blood glucose in diabetics can cause hyperactivity in the polyol metabolic pathway [3-5]. This pathway involves 2 enzymes, known as aldose reductase [6,7] and sorbitol dehydrogenase [8]. The first stage in this pathway is NADPH-dependent catalysis by the enzyme aldose reductase to reduce glucose to sorbitol. In the second stage, the sorbitol dehydrogenase will oxidize sorbitol to fructose along with the coenzyme NAD^+ to NADH [9]. The high activity of the aldose reductase in the polyol pathway is associated with various pathogenic factors, which in the long term will cause secondary complications in patients with diabetic mellitus. Sorbitol does not readily diffuse through cell

membranes. Therefore sorbitol accumulating in cells will cause hypertonicity followed by osmotic stress, then contributing to diabetic complications, such as nephropathy, neuropathy, and retinopathy [10-12]. Aldose reductase inhibitors (ARIs) can inhibit the polyol pathway and be used as antidiabetic therapy to avoid and slow the development of diabetes complications. Several ARIs have been used for antidiabetic drugs, such as fidarestat, tolrestat, and sorbinil [13,14]. However, these ARIs cause side effects toxicity [15]. Therefore, discovering new agents with more diverse and safe structures became an interesting and profound goal for developing antidiabetic therapies.

Currently, research on synthesis of pyridazinone derivatives is often studied. The pyridazinone derivatives showed pharmacophore effects, such as cardioactive agents [16,17], anticancer [18,19], anti-bacterial [20], antimycobacterial [21], COX-2 inhibitors and anti-inflammatory [22-24], and antioxidants [25]. Previous studies have found that 6-substituted-3(2H)-pyridazinone-2-ylacetate derivatives showed cholinesterase inhibitory Ozdemir *et al.* [26] and vasodilator activity [27]. Pyridazinone derivatives have also been shown to be potent against α-glucosidase enzyme [28].

Synthesis of pyridazinone derivatives 4a - 4d have been carried out using substituted-acetophenone, glyoxylic acid, and hydrazine Krasavin *et al.* [29] through a one-pot process using a heating reactor. A phenyl group of acetophenone bound with a pyridazinone ring was designed for a methoxy group as the electron-donating group, then chlorin and bromo as electron-withdrawing. The effect of these substituted groups and their position on the phenyl ring will be considered to analyze their pharmacology effects. Next, for the synthesis of compound 5 and 6a - 6d, modifications were made such as substituting hydrogen at position 2 of the pyridazinone ring with benzene sulphonyl chloride and ethyl acetate groups. The substituted-3(2H)-pyridazinone-2-ylacetate derivatives (6c and 6d) have been synthesized before [27,30]. However, the 6a, 6b, and 5 compounds have never been reported.

The inhibitors of ARIs have multiple structures, but some common features can be identified, basically being divided into 3 main classes of classical inhibitors: compounds that contain cyclic imides, carboxylic-acid derivatives, and polyphenolic compounds [31]. However, many studies have also shown that the structure of ARI inhibitors can be further developed. Novel acyl hydrazone derivatives were looked at as AR enzyme inhibitors. They were very effective, 17.38- and 10.78-fold more effective than the standard drug epalrestat. This is in line with the results of molecular docking studies. Additionally, this compound exhibits safe ADME properties [32]. Several derivatives of compounds containing sulfonate groups have been studied to have properties as effective aldose reductase inhibitors. Askarova [33] has synthesized compounds containing sulfonate groups, specifically sulfamidomethylation derivatives of phenols, which exhibit activity as aldose reductase inhibitors. Additionally, non-acidic 4-methylbenzenesulfonate inhibited the ALR2 enzymatic activity in a sub micromolar *in vitro* setting and was found to be non-toxic [34]. The study's findings on sulfides and sulfones could be exploited to create innovative therapeutics that prevent diabetes complications. According to the ADME-Tox study, these compounds are predicted to be ALR2s with appropriate drug-like characteristics [35].

Based on the above studies, all the synthesized pyridazinone derivatives were tested to see if they could work as aldose reductase enzyme inhibitors to help treat complications that come up with diabetes mellitus. There were molecular docking studies done on the synthesized pyridazinone derivatives to predict the binding free energy and conformation binding. Furthermore, a detailed understanding of *in silico* pharmacokinetic prediction (ADMET) was carried out to support the discovery of a drug design for diabetic complications therapy.

In contrast to previous studies, the current research introduces a more efficient synthesis of pyridazinone derivatives through a one-pot method using a heating reactor. The pyridazinone synthesis method was modified using the one-pot method in a monowave reactor tube. Hydrazine was directly added to the reactor tube after the reaction between glyoxylic acid and acetophenone took place for 2 - 3 h without going through the purification of the intermediate oxobutanoic acid compound. This method is more efficient because it can save solvents. In previous studies, the synthesis of pyridazinone was carried out through 2 reaction stages [29,36]. In this study, the synthesis of pyridazinone

using a monowave accelerated the reaction compared to the traditional stirred hot-plate setup. This was due to the use of a tightly fitted, electrically heated metal heating jacket, which mimicked the heating rate of a microwave reactor. Other researchers have never used monowave to synthesize pyridazinone.

Materials and methods

Materials

The materials that were used for this research were glyoxylic acid ($C_2H_2O_3$), methoxy acetophenone ($C_9H_{10}O_2$), glacial acetate acid (CH_3COOH), hydrazine monohydrate ($N_2H_4•H_2O$), sodium hydroxide (NaOH), 6-(3-bromophenyl)pyridazine-3(2H)-on ($C_{10}H_7BrN_2O$), benzene sulfonyl chloride ($C_6H_5SO_2Cl$), potassium carbonate (K_2CO_3), acetonitrile (C_2H_3N), and ethyl chloroacetate ($C_4H_7ClO_2$). All materials were purchased from Merck and Sigma-Aldrich. The materials were used without purification.

Equipment and instrumentation

The synthesis reaction was carried out using a Monowave 50 heating reactor(Anton-Paar, Graz, Austria). The melting point was obtained by a Fisher-Johns apparatus (Fisher Scientific, Waltham, MA, USA) (uncorr). Thin Layer Chromatography (TLC) analysis was carried out using GF254 (Merck Millipore, Darmstadt, Germany) under a UV lamp 254/365 nm (Cole-Elmer®, Vernon Hills, IL, USA). The FT-IR spectra, Mass spectra, and 1H-NMR spectra was recorded in KBr powder on a Shimadzu® FT-IR Prestige-21 spectrophotometer (Shimadzu Corporation, Kyoto, Japan), Water Xevo QTOFMS instrument (Waters, Milford, MA, USA), and an Agilent® (Agilent Technologies, Santa Clara, CA, USA), respectively. The molecular docking analysis was performed using the MOE 2020.0102 software package and Discovery Studio Visualizer (DSV) 2019 software.

Synthesis of 6-(2/3/4methoxyphenyl)-pyridazinone-3(2H)-one (4a-4d)

Synthesis of 6-(substituted phenyl)-pyridazinone-3(2H)-ones (4a - 4d) were carried out based on Cruz *et al.* method [37], but modified for one-pot method. A mixture of glyoxylic acid (3 mmol), methoxy acetophenone (3 mmol), and glacial acetate acid (3 mL) were mixed in a heating reactor at 120 °C for 3 h. After that, hydrazine monohydrate (3 mmol) was added to the mixture and the reactor was set at 80 °C for 2 h. Next, 40 % of sodium hydroxide (NaOH) was added to the mixture for the neutralization process. The precipitate formed was filtered and washed. The solid products are recrystallized in methanol to obtain compounds 4a - 4d. Crystal purity test was carried out by HPLC analysis, TLC, and melting point determination. Each compound was characterized by spectroscopy methods IR, MS, and 1H-NMR.

6-(2-methoxyphenyl)-pyridazin-3(2H)-one (4a)

Molecular formula $C_{11}H_{10}N_2O_2$, brown dark solid (46.86 % yield). m.p. 130 - 131 °C HPLC chromatogram tR = 17.321 min. FT-IR spectrum (KBr) $\bar{U}$ (cm^{-1}): 3,198 cm^{-1} (N-H amine), 2,865 cm^{-1} (C-H sp^3), 1,678 cm^{-1} (C=O), 1,593 cm^{-1} (C=N). ^{1}H-NMR (500 MHz, $CDCl_3$) δ (ppm): 11.76 (s, 1H), 7.78 (d, *J* = 9.8 Hz, 1H), 7.59 (dd, *J* = 7.6, 1.8 Hz, 1H), 7.42 (ddd, *J* = 8.3 Hz, 7.4, 1.8 Hz 1H), 7.06 (td, *J* = 7.5, 1.1 Hz, 1H), 7.00 (d, *J* = 8.3 Hz, 1H), 6.97 (d, *J* = 9.8 Hz, 1H), 3.88 (s, 3H). HRMS (ESI): m/z 203.0825 $[M + H]^+$ (calcd. for $C_{11}H_{10}N_2O_2$: 203.0821).

6-(3-methoxyphenyl)-pyridazin-3(2H)-one (4b)

Molecular formula $C_{11}H_{10}N_2O_2$, light brown solid (72.60 % yield). m.p. 135 - 136 °C. HPLC chromatogram tR = 4.566 min (254 nm) and 4.558 min (365 nm). FT-IR spectrum (KBr) $\bar{U}$ (cm^{-1}): 3,204 cm^{-1} (N-H amine), 2,923 cm^{-1} (C-H sp^3), 1,661 cm^{-1} (C=O), 1,595 cm^{-1} (C=N). ^{1}H-NMR (500 MHz, $CDCl_3$) δ (ppm): 11.42 (s, 1H), 7.77 (d, *J* = 9.9 Hz, 1H), 7.40 (d, *J* = 7.9 Hz, 1H), 7.38 (s, 1H), 7.34 (dt, *J* = 7.9, 1.2 Hz, 1H), 7.08 (d, *J* = 9.9 Hz, 1H), 7.00 (dd, *J* = 8.1, 2.4 Hz, 1H), 3.89 (s, 3H). HRMS (ESI): m/z 203.0817 $[M + H]^+$ (calcd. for $C_{11}H_{10}N_2O_2$: 203.0821).

6-(4-methoxyphenyl)-pyridazin-3(2H)-one (4c)

Molecular formula $C_{11}H_{10}N_2O_2$, brown solid (81.84 % yield). m.p. 148 - 149°C. HPLC chromatogram tR = 4.586 min (254 nm) dan 4.558 (365 nm). FT-IR spectrum (KBr) $\bar{U}$ (cm^{-1}): 3,201 cm^{-1} (N-H amine), 2,908 cm^{-1} (C-H sp^3), 1,655 cm^{-1} (C=O), 1,593 cm^{-1} (C=N). ^{1}H-NMR (500 MHz, $CDCl_3$) δ (ppm): 11.55 (s, 1H), 7.74 (d, *J* = 8.5 Hz, 2H), 7.74 (d, *J* = 10.0 Hz, 1H), 7.06 (d, *J* = 10.0 Hz, 1H), 6.99 (d, *J* = 8.5 Hz,

2H), 3.87 (d, *J* = 1.0 Hz, 3H). HRMS (ESI): m/z 203.0826 $[M + H]^+$ (calcd. for $C_{11}H_{10}N_2O_2$: 203.0821).

6-(3-bromophenyl-pyridazin-3(2H)-one (4d)

Molecular formula $C_{10}H_7BrN_2O$, brown solid (98.4 %). m.p. 117 - 118 °C. HPLC chromatogram tR = 5.787 min (λ = 254 nm). FT-IR spectrum (KBr) Ū (cm^{-1}): 3,126 cm^{-1} (N-H amine), 1,707 cm^{-1} (C=O), 1,585 cm^{-1} (C=N), 1,288 cm^{-1} (C-N), 591(C-Br). ^{1}H-NMR (500 MHz, $CDCl_3$) δ (ppm): δ 10.93 (s, 1H), 7.96 (s, 1H), 7.76 - 7.68 (m, 2H), 7.59 (d, *J* = 8.2 Hz, 1H), 7.36 (t, *J* = 7.9 Hz, 1H), 7.09 (d, *J* = 9.9 Hz, 1H). HRMS (ESI): m/z 250.9820 $[M+H]^+$ (calcd. For $C_{10}H_7BrN_2O$: 250.9820).

Synthesis of 6-(3-bromophenyl)-2-(phenylsulfonyl)pyridazine-3(2H)-one (5)

Synthesis of 6-(3-bromophenyl)pyridazine-3(2H)-on (5) was carried out based on Kweon *et al*. method, but modified for one-pot method [38]. The mixtures of compounds 6-(3-bromophenyl)pyridazine-3(2H)-on (1 mmol), benzene sulfonyl chloride (2 mmol), potassium carbonate (2.5 mmol), and acetonitrile (15 mL) were stirred for 8 h at room temperature and the synthesis progress was controlled using TLC. The solid was extracted using a solvent system of 50 % ethyl acetate: distilled water. The ethyl acetate layer was collected to obtain the purified compound **5**. The purity of the product was using the TLC, melting point determination, and HPLC test.

6-(3-bromophenyl)-2-(phenylsulfonyl)pyridazine-3(2H)-one (5)

Molecular formula $C_{16}H_{12}BrNO_3S$, white (15.66 % yield), m.p. 157 - 158 °C HPLC Chromatogram tR = 7.244 (250 nm. FT-IR spectrum (KBr) Ū (cm^{-1}): 3,067 cm^{-1} (C-H aromatic), 1,707 cm^{-1} (C=O), 1,609 cm^{-1} (C=N), 1,194 cm^{-1} (SO_2), 689 cm^{-1} (C-Br).^{1}H-NMR (500 MHz, $CDCl_3$) δ (ppm): δ 8.23 (d, *J* = 7.3 Hz, 2H), 7.98 (s, 1H), 7.79 (d, *J* = 8.3 Hz, 1H), 7.72 (t, *J* = 7.5 Hz, 1H), 7.66 (d, *J* = 9.8 Hz, 1H), 7.64 - 7.56 (m, 3H), 7.38 (t, *J* = 7.9 Hz, 1H), 6.96 (d, *J* = 9.8 Hz, 1H). ^{13}C NMR (126 MHz, $CDCl_3$) δ (ppm): 157.27, 143.30, 136.28, 135.60, 135.00, 133.34, 132.86, 131.52, 130.62, 129.90, 129.39, 129.05, 124.97, 123.35. HRMS (ESI) (m/z): 390.9758 $[M+H]^+$. (Calcd. for $C_{16}H_{12}BrNO_3S$: 390.9759).

Synthesis of ethyl-2-(3-(-substituted phenyl)-6-oxopyridazine 1(6H)-il) acetate (6a-6d)

Ethyl 2-(3-(-substituted phenyl)-6-oxopyridazine-1(6H)-il) acetate (6a-6d) were carried out by modifying the procedure proposed by Allam *et al.* [27] with one-pot method. Each mixture of appropriate compounds 4a - 4d (0.01 mol) and K_2CO_3 (0.02 mol) was added ethyl chloroacetate (0.015 mol) dropwise while stirring with a magnetic stirrer for 2 - 3 h at 400 RPM, room temperature and controlled using TLC. Next, the mixture is poured into a container filled with ice cubes and continuously stirred. The precipitate was filtered and washed. The product solids are recrystallized in methanol to obtain compounds 6a - 6d. Crystal purity test was carried out by HPLC analysis, TLC, and melting point determination. The crystal structure was characterized by spectroscopy methods IR, MS, and 1H-NMR.

Ethyl-2-(3-(2-metoxyphenyl)-6-oxopyridazine 1(6H)-il)acetate (6a)

Molecular formula $C_{15}H_{16}N_2O_4$, fawn-colored solid (33.33 % yield). m.p. 166 - 168 °C HPLC Chromatogram tR = 4.573 min (254 nm) and 4.575 min (365 nm). FT-IR spectrum (KBr) Ū (cm^{-1}): 2,992 cm^{-1} (C-H sp^3), 1,741 dan 1,674 cm^{-1} (C=O), 1,592 cm^{-1} (C=N), 1,220 cm^{-1} (C-O). ^{1}H-NMR (500 MHz, $CDCl_3$) δ 7.74 (d, *J* = 9.7 Hz, 1H), 7.56 (dd, *J* = 7.6, 1.8 Hz, 1H), 7.42 (td, *J* = 7.9, 1.7 Hz, 1H), 7.05 (t, *J* = 7.5 Hz, 1H), 6.99 (d, *J* = 8.3 Hz, 1H), 6.95 (d, *J* = 9.7 Hz, 1H), 4.96 (s, 2H), 4.26 (q, *J* = 7.1 Hz, 2H), 3.87 (s, 3H), 1.31 (t, *J* = 7.1 Hz, 3H). HRMS (ESI) (m/z): 289.1174 $[M+H]^+$. (Calcd. for $C_{15}H_{16}N_2O_4$: 289.1188).

Ethyl-2-(3-(3-metoxyphenyl)-6-oxopyridazine 1(6H)-il)acetate (6b)

Molecular formula $C_{15}H_{16}N_2O_4$, yellow solid (74.65 % yield). mp 58 - 59 °C HPLC Chromatogram tR = 4.542 min (254 nm) and 4.543 min (365 nm). FT-IR spectrum (KBr) Ū (cm^{-1}): 2,945 cm^{-1} (C-H sp^3), 1,753 dan 1,673 cm^{-1} (C=O), 1,599 cm^{-1} (C=N), 1,214 cm^{-1} (C-O). ^{1}H-NMR (500 MHz, $CDCl_3$) δ 7.71 (d, *J* = 9.7 Hz, 1H), 7.38 (t, *J* = 7.9 Hz, 1H), 7.33 (s, 1H), 7.33 (d, *J* = 8.4 Hz, 1H), 7.06 (d, *J* = 9.7 Hz, 1H), 6.99 (dt, *J* = 8.1, 1.5 Hz, 1H), 4.98 (s, 2H), 4.27 (q, *J* = 7.1 Hz, 2H), 3.88 (s, 3H), 1.31 (t, *J* = 7.1 Hz, 3H). HRMS (ESI)

(m/z): 289.1187 $[M+H]^+$. (Calcd. for $C_{15}H_{16}N_2O_4$: 289.1188).

Ethyl-2-(3-(4-metoxyphenyl)-6-oxopyridazine 1(6H)-il)acetate (6c)

Molecular formula $C_{15}H_{16}N_2O_4$, yellow solid (88.9 % yield). m.p. 91 - 92 °C HPLC Chromatogram tR = 4.286 min (254 nm) and 4.288 min (365 nm). FT-IR spectrum (KBr) Ū (cm^{-1}): 2,988 cm^{-1} (C-H sp^3), 1,758 dan 1,667 cm^{-1} (C=O), 1,576 cm^{-1} (C=N), 1,212 cm^{-1} (C-O). ^{1}H-NMR (500 MHz, $CDCl_3$) δ (ppm): δ 7.72 (d, *J* = 9.0 Hz, 2H), 7.69 (d, *J* = 10.0 Hz, 1H), 7.04 (d, *J* = 10.0 Hz, 1H), 6.98 (d, *J* = 8.5 Hz, 2H), 4.96 (s, 2H), 4.27 (q, *J* = 7.1 Hz, 2H), 3.86 (s, 3H),1.30 (t, *J* = 7.1 Hz, 3H). HRMS (ESI) (m/z): 289.1189 $[M+H]^+$ (Calcd. for $C_{15}H_{16}N_2O_4$: 289.1188).

Ethyl-2-(3-(3-bromophenyl)-6-oxopyridazine 1(6H)-il)acetate (6d)

Molecular formula $C_{14}H_{14}N_2O_3Br$, light brown solid (91.04 % yield). m.p. 89 - 90 °C HPLC Chromatogram tR = 15.445 (254 nm). FT-IR spectrum (KBr) Ū (cm^{-1}): 2,978 cm^{-1} (C-H sp^3), 1,742 dan 1,690 cm^{-1} (C=O), 1,590 cm^{-1} (C=N), 1,220 cm^{-1} (C-O), 578 cm^{-1} (C-Br). ^{1}H-NMR (500 MHz, $CDCl_3$) δ (ppm): δ 7.96 (s, 1H); 7.70 (d, *J* = 9.7 Hz, 1H); 7.69 (d, *J* = 8.2 Hz, 1H), 7.57 (d, *J* = 8.0 Hz, 1H); 7.34 (t, *J* = 7.9 Hz, 1H); 7.08 (d, *J* = 9.7 Hz, 1H); 4.98 (s, 2H); 4.28 (q, *J* = 7.1 Hz, 2H); 1.32 (t, *J* = 7.1 Hz, 3H). HRMS (ESI) (m/z): 337.0188 $[M+H]^+$ (Calcd. for $C_{14}H_{14}N_2O_3Br$: 337.0188).

Molecular Docking

Ligand and receptor preparation

The crystal structure of the selected receptor was downloaded from the protein database (https://www.rcsb.org/), namely the aldose reductase receptor (PDB ID 1Z89 with resolution 1.43 Å) in the bound state with sulfonyl-pyridazinone inhibitor [39]. Molecular docking was performed using Molecular Operating Environment (MOE). The receptor was prepared by adding all hydrogen atoms and adjusting the total charge of the residues during the structure preparation process. Receptor preparation was done by minimizing energy by selecting the CHARMM27 force field, determining the coordinates of the receptor-ligand interaction center (wall), and setting the RMS gradient to 0.01 kcal/mol/Å. CHARMM27 force fields are used in research to minimize the energy of the aldose reductase enzyme protein because they are commonly used in all-atom proteins, DNA, and RNA.

Pyridazinone derivatives and the positive control, tolrestat, served as ligands. The prepared ligands comprised the formation of a 3-dimensional structure, the additional hydrogen atoms, and the estimation of partial charges. The energy of molecules was minimized by implementing force field MMF94x until the RMS gradient of 0.001 kcal/mol/Å. The Merck Molecular Force Field (MMFF94) is a commonly used force field equation for energy minimization in small organic molecules in medicinal chemistry. For docking, the parameters were set for score selection using the London dG scoring function, and for method selection using the Triangle Matcher protocol for placement and Rigid Receptor for refinement. The lowest binding free energy (S-score, in kcal/mol) was selected for analysis. The results of docking were visualized using MOE 2020.0101 software.

Docking

The MOE 2020.0901 (Chemical Computing Group) software was used to examine the molecular interaction. Before initiating the docking procedure, the active site of the protein was identified using a site finder, comprising several amino acid residues. This site was designated as a dummy atom to serve as the target location for the docking process. In the docking menu, the site was configured as a dummy atom, and the prepared ligand structure, saved in an MDB file, was selected. The placement parameters were set to a triangular configuration, refinement was specified as rigid, and the pose values were established at 100 and 10, respectively. Once the folder for storing the docking results was selected, the "Run" button was clicked, and the docking process was awaited until its completion.

The prediction of drug-likeness and absorption, distribution, metabolism, excretion, and toxicity (ADMET)

The prediction of drug-likeness was conducted using the SwissADME website (http://www.swissadme.ch/index.php). The parameters were analyzed to ensure the Lipinski Rule of 5, namely molecular weight (≤ 500); molar refractivity (40 - 130);

hydrogen bond acceptor (≤ 10); hydrogen bond donor (≤ 5); lipophilicity (as LogP, ≤ 5).

ADME profiles were generated using the pre-ADME tool (https://preadmet.webservice.bmdrc.org/). The selected endpoints in pre-ADME were Blood Brain Barrier (BBB), Human Intestinal absorption (HIA), Plasma Protein Binding (PPP), skin permeability, Caco-2 cell permeability, and cytochrome P450. The toxicity profiles were performed using ProTox II (https://tox-new.charite.de/). The selected endpoints in ProTox II were mutagenicity, hepatoxicity, immunotoxicity, carcinogenicity, rat acute oral toxicity (LD_{50}), and toxicity classification.

Results and discussion

The synthesis of 4a - 4d was carried out by one-pot method using heating reactor through a cyclocondensation reaction between substituted-acetophenone, glyoxylic acid, hydrazine, and carboxylic acid as a catalyst. Here, the synthesis process of 4a - 4d by one-pot method using heating reactor was proven more effective and safer. The heating reactors based on the conventional heating principle have adequate process control in a sealed vessel reactor, namely: heating and cooling performance at 250 °C and pressure control in addition to magnetic stirring efficiency [40]. Conversely, the one-pot method conserves solvents as it bypasses the extraction process of the oxobutanoic acid intermediate product, unlike previous studies. Previous studies have reported the synthesis of pyridazinone derivatives using reflux heating for 4 - 8 h, which involves more reaction steps and solvents. Specifically, after the formation of the intermediate compound in the first stage, extraction is carried out to obtain a pure oxobutanoic acid intermediate compound. Next, hydrazine hydrate is added to produce the pyridazinone ring product [29,36]. The one-pot synthesis method does not need to extract the oxobutanoic acid intermediate compound, but the hydrazine compound is directly added into the reactor tube to form its pyridazinone ring product leading to enhanced efficiency and faster synthesis process. Therefore, the one-pot synthesis method is more effective, energy-efficient, and safer for the environment compared to the conventional method.

The basic principle of pyridazinone synthesis is the condensation reaction 1,2-dicarbonyl (a ketone containing the active groups of methylene) with hydrazine. In the first step, an aldol condensation reaction occurred between the ketone group) and glyoxylic acid 2 using a glacial acetic acid catalyst to produce oxobutanoic acid intermediate 3. Then in the second step, the addition of hydrazine causes an intramolecular cyclization reaction in which the nucleophilic nitrogen atom attacks the carbonyl carbon of oxobutanoic acid to reduce the pyridazinone derivative. The synthetic pathway 4a - 4d is depicted in **Figure 2**.

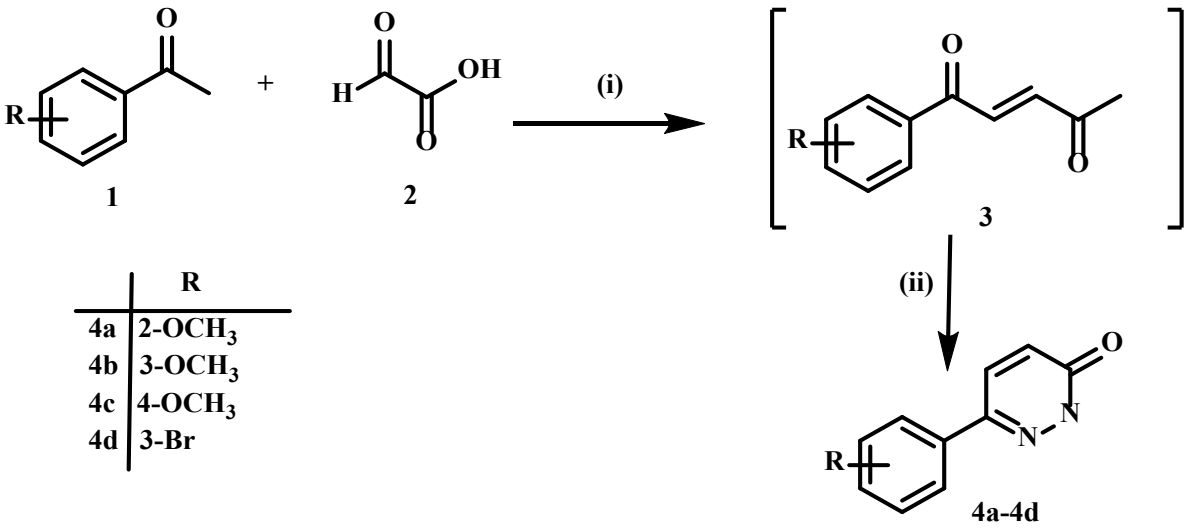

Figure 2 Synthesis route of 4a - 4d. Reagent and condition: (i) AcOH as the catalyst, heated at 120 °C, 3 h (ii) Hydrazine hydrate, heated at 80 °C, 2 h.

In general, the IR spectra of the 4a - 4d derivatives showed similar absorption bands at wave numbers according to the presence of functional groups in the compounds. The IR spectrum indicated the presence of functional groups at corresponding wavenumbers around in the range of 1,651 - 1,678 cm^{-1} (C=O stretching), 1,593 to 1,595 cm^{-1} (C=N stretching), 2,865 - 2,923 cm^{-1} (C-H sp3 bond stretching), 3,198 - 3,204 cm^{-1} (N-H bond). The absorption band at 687 cm^{-1} indicated C-Br vibration of the compound 4d.

The ^{1}H-NMR spectrum shows almost the same chemical shift in compounds 4a - 4d that indicated the typical peak signal of the pyridazinone ring that appears at a suitable chemical shift, namely the protons Hα and Hβ with a doublet peak orientation respectively. The protons Hα at δH 6.97 - 7.08 ppm and Hβ at δH 7.74 - 7.78 ppm, while J coupling ranging from 9.8 to Hz. In addition, the analysis result revealed that one singlet proton signal appeared at δH 11.42 - 11.76 ppm, confirming protons of nitrogen atoms of the pyridazinone ring. Indeed, The pattern is consistent with observations made by Cruz and coworkers [37] for 3-(2H) pyridazinones. All the aromatic proton signals were observed at δH 6.99 - 7.73 ppm. The protons of substituent $-OCH_3$ of 4a - 4c exhibited a singlet peak located in the downfield area at δH 3.87 - 3.89 ppm.

Subsequently, 4a - 4d compounds were reacted with ethyl acetate in the present K_2CO_3 as a catalyst to get 6a - 6d compounds. K_2CO_3 is a heterogeneous base catalyst that can increase the nitrogen nucleophilic properties, causing the release of the leaving groups. Then, compound 5 was obtained by substitution of the hydrogen atom of 4d with benzene sulphonyl chloride. Mechanism reactions for the formation of 5 and 6a - 6d compounds are outlined in **Figure 3**.

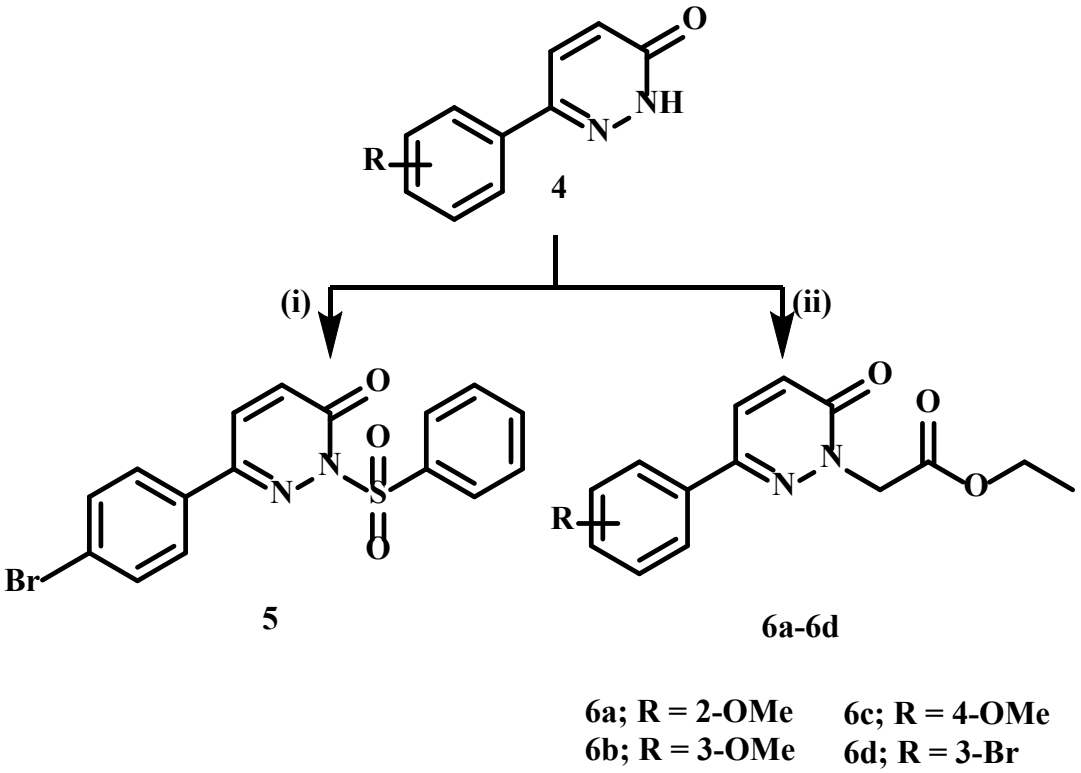

Figure 3 Synthesis route of pyridazinone derivatives compound 5 and 6a - 6d. Reagent and condition: (i) $C_6H_5SO_2Cl$, K_2CO_3, CH_3CN, stirrer in rt, 8 h; (ii) Ethyl chloro acetate, K_2CO_3, stirring in RT, 2 - 3 h.

The IR spectrum generally showed absorption by the functional groups present in the target compounds. An essential indicator in the spectrum was the loss of absorption of the NH group at wavelengths > 3,100 cm^{-1}. The compounds 6a - 6d keep 2 C=O bond stretching vibration groups, both of the pyridazinone ring and the aliphatic ester chain were observed at about 1,738 - 1,758 cm^{-1} and 1,673 - 1,690 cm^{-1}, respectively. The absorption band at 1,212 - 1,293 cm^{-1} indicated the C-O stretching of the ester. The IR spectroscopy shows

several peaks and typical bond vibrations for compound 5 that wave number 1,194.95 cm^{-1} indicating the SO_2 bond vibration attached to the pyridazinone ring. The vibration of the C-Br bond at wave number 689.58 cm^{-1}. The spectrum HRMS of all compounds is displayed at the appropriate calculated molecular mass and the molecular mass.

Compounds 5 and 6a - 6d were successfully synthesized as evidenced by the loss of the NH proton peak on H-NMR. The loss of the NH proton peak is due to a substitution reaction with the ethyl chloro acetate (**Figure 2**). The peak signal of the protons Hα and Hβ on the pyridazinone ring are in good agreement which exhibited a doublet peak orientation at a chemical shift of approximately at δH 6.95 - 7.07 ppm and δH 7.71 - 7.74, respectively. The signal belonging to the CH_3 group of the aliphatic ester chain was observed in the aliphatic region at δH 1.30 - 1.32 ppm with triplet orientation. Meanwhile, protons in the CH_2 group of the aliphatic ester chain resulted at δH 4.26 - 4.28 ppm in a quartet orientation. The induction effect of the nitrogen atom and the carbonyl group caused the protons of the methylene-bound nitrogen to be most deshielding in the other protons in the aliphatic ester chain. It appears at δH 4.97 - 4.98 ppm with singlet orientation.

Molecular docking results

A study using molecular docking was done on the aldose reductase enzyme (PDB ID: 1Z89), which is the crystal structure of human aldose reductase combined with the sulfonyl-pyridazinone inhibitor [39]. The 1Z89 receptor was chosen as the target because the native ligand is a pyridazinone derivative containing an SO_2 group, and this structure is consistent with the target compound. Molecular docking was performed to position ligands at the desired binding sites of the receptor. The antagonist activity of the synthesized pyridazinone derivatives against aldose reductase was assessed based on their binding free energy values and the types of interactions with the aldose reductase enzyme. The docking process is carried out around the active site where the native ligand is located. These active sites corresponded to Cachau *et al.* [41] study, who reported that there are the active site residues (Trp111, Tyr48, and His110) performed hydrogen bonds between the inhibitor and AR2, and other residues (Trp20, Trp79, Asp43, Ser159, Gln183, Asnl60, and Tyr209, Cys298, Tyr309, and Trp219) allow to the shape of the active site.

The docking protocol was validated by redocking the sulfonyl-pyridazinone native ligand, which exhibited a binding free energy of −11.93 kcal/mol and an RMSD of 1.34. The RMSD value of the redocked ligand, bein ≤ 2, indicates that the docked ligand is similar to the position of the native ligand, suggesting that this method can be reliably used as a docking protocol. This is further supported by the superimposition of the native ligand with the sulfonyl-pyridazinone ligand pose, demonstrating the similarity in the binding pose of the redocked ligand with the native co-crystal ligand at the active site residues of aldose reductase. The superimposition of the native ligand and the redocked ligand pose of the sulfonyl-pyridazinone is shown in **Figure 4**.

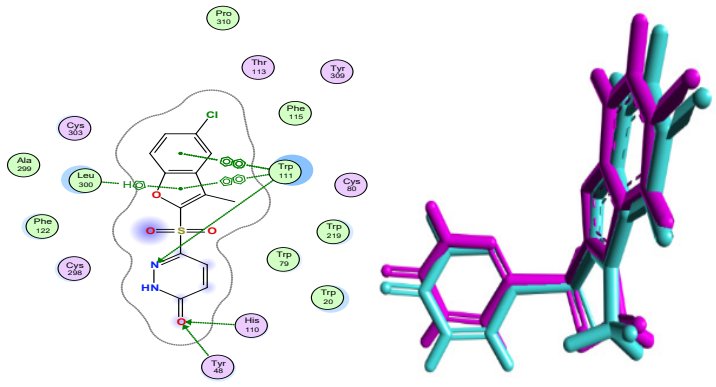

(a) (b)

Figure 4 (a) Visualization of the binding mode of native ligand sulfonyl-pyridazinone (b) Superimposition between native ligand (pink) and redocked-ligand of sulfonyl-pyridazinone (cyan).

The binding free energy values for pyridazinone derivatives are depicted in **Table 1**. The free energy value of compounds 4a - 4d, 5, and 6a - 6d showed that they have lower potential inhibitory activity against the aldose reductase enzyme than the positive tolrestat control (−14.12 kcal/mol). Compound 5 exhibited the lowest binding free energy value (S = −12.61 kcal/mol). The docking score value chosen for this study was the one with the lowest score among all the target ligands compared to the positive control (tolrestat). Compound 5 has a docking score close to the tolrestat value. So, it is predicted that compound 5 has the best activity compared to other ligands. The binding free energy value is related to the strength of the bond formed between the ligand and its receptor. The smaller the binding free energy value, the stronger and more stable the bond formed between the ligand and the receptor [42]. Based on **Table 1**, the docking visualization results showed that the positive control tolrestat has 19 contact residues on the active site of the receptor, namely Trp111, His110, Phe122, Tyr48, Cys80, Phe115, Trp79, Thr113, Tyr209, Lys77, Gln183, Asn160, Trp20, Cys298, Trp219, Ala299, Cys303, Tyr309, Leu300. Tolrestat as positive control interacts with the receptor via 2 hydrogen bonds with Tyr48 and His 110 residues and one hydrophobic bond (π-π stacking contact) with Trp111 residue. According to Urzhumtsev *et al.* [43], tolrestat is an aldose reductase inhibitor that contains a polar head of the COOH group. This head may interact with residues Trp111, His110, and Tyr48 through hydrogen bonds where it is shared between C=O and OH at the bottom of the AR active site. Compound 4a formed one hydrogen bond with His110 and one hydrophobic bond (π-H stacking contact) with Trp111. Compounds 4b and 4d interact with important residues in the process of blocking aldose reductase, or they act similarly to how tolrestat positive controls interact. Each of these compounds formed 2 hydrogen bonds with His 110 and Tyr48 and one hydrophobic bond (π-π stacking contact) with Trp111.

Table 1 The docking result of pyridazinone derivatives.

Comp	Binding free energy (kcal/mol)	RMSD	Bond type			Factor of bond
			Hydrogen bond	Hydrophobic bond	Other interaction	
4a	−9.53	1.05	His110	Trp111	Asp43, Ile260, Tyr209, Lys77, Gln183, Tyr48, Ser159, Asn160, Trp79, Trp219, Cys298, Trp20	11
4b	−9.67	0.89	Tyr48, His110	-	Trp111, Trp20, Ala299, Leu300, Trp219, Cys298, Trp79	9
4c	−9.60	0.67	Asp43	His110, Tyr209	Tyr48, Trp111, Cys298, Trp79, Trp20, Asn160, Ser210, Gly18, Ile260, Gln183, Lys77	10
4d	−9.43	1.28	Tyr48, His110	Trp20, Trp111	Val47, Trp219, Leu300, Ala299, Trp79, Cys298	9
5	−12.61	0.76	Tyr48, His110, His110, Cys298, Asn160	Trp111, His110, Tyr209	Ile260, Trp20, Val47, Trp79, Trp219, Asp43, Leu300, Lys77, Ala299, Gln183	13
6a	−12.20	1.93	Tyr48, His110	Trp20, Trp111	Tyr209, Gln183, Val47, Phe122, Trp79, Cys298, Ala299, Leu300, Trp219	15
6b	−12.00	1.09	Tyr48, His110	Trp20, Trp111	Tyr209, Gln183, Val47, Thr113, Trp79, Phe115, Phe122, Cys80, Cys303, Leu300, Ala299	15
6c	−11.73	2.40	Tyr48, His110	Trp20, Trp111	Cys298, Asn160, Ser159, Gln183, Tyr209, Phe122, Leu300, Pro310, Cys303, Ala299	13
6d	−12.01	1.55	Tyr48, His, 110	Trp20, Trp111	Cys298, Tyr209, Val47, Ser159, Asn160, Gln183, Trp79, Phe122, Thr113, Cys303, Phe115, Leu300, Ala299	15
Tolrestat	−14.13	1.87	Tyr48, His110	Trp111	Phe122, Cys80, Phe115, Trp79, Thr113, Tyr209, Lys77, Gln183, Asn160, Trp20, Cys298, Trp219, Ala299, Cys303, Tyr309, Leu300	-

Compound 5 exhibited the lowest binding free energy value (S = −12.61 kcal/mol), indicating that it has a high binding affinity and forms a more stable interaction with the receptor compared to other target compounds. The strength of the bond formed between the ligand and its receptor is directly related to the lowest-bidding free energy. The smaller the value of the binding free energy, the stronger the bond formed between the ligand and the receptor. In this study, the docking score value selected was based on the docking score value compared to the positive control (tolrestat). The tolrestat value has binding free energy value of −14.13 kcal/mol, while compound 5 has a docking score that is close to the tolrestat value. So, it is predicted that compound 5 has the best activity compared to other ligands. This result is also supported by the pose of the interaction that occurs, in which compound 5 formed 5 hydrogen bonds with residues Tyr48, His110, His110, Cys298, and Asn160, and 3 hydrophobic bonds, namely π-H stacking contact interactions with Trp111 and His110, as well as one π-π interaction stacking contact with Tyr209. Additionally, the carbonyl group in SO_2 can improve the compound's electronic properties, thereby increasing the hydrogen bonding interactions. The more hydrogen bonds, the stronger the ligand-receptor complex formation. In addition, the geometric tension due to the interaction of hydrogen bonds makes the ligand transfer more effective [44]. This conformation indicates that compound 5 has the potential to be an aldose reductase inhibitor because it can bind to important residues for inhibitor activity (Tyr48, His110, His110, Cys298, Trp 111). Meanwhile, Trp20 and Cys80 are not important residues, so whether or not the ligand binds to them does not significantly affect activity. This binding mode is in accordance with that reported by Cachau *et al.* [41]. Hodoscek [45] has also reported the binding modes of 6 aldose reductase inhibitors that also form binding conformations with the critical residues Tyr48, His110, and Trp111; the combination of hydrogen bonding and aromatic-aromatic interactions has been attributed to playing a major role in enhancing the binding affinity of ARIs. Salem *et al.* [46] found that compounds 12B and 15C were potent antagonists for ALR2 over ALR1, *both in vitro* with IC50s of 0.29 and 0.35 μM, and they were more potent than the standard ALR2 inhibitor epalrestat with an IC50 of 0.40 μM. This result was supported by molecular docking studies, where these compounds formed bonds with residues His110, Tyr48, and Trp111. Furthermore, the given results are in line with the binding conformation that occurs in the sulfonyl-pyridazinone native co-crystal ligand, which forms 3 hydrogen bonds with His110, Tyr48, and Trp111, as well as 3 hydrophobic bonds with Trp111, Trp111, and Leu30017 (**Figure 4**). It also is confirmed by the previous research that hydrogen bonding was established between Tyr48 and His110 and the carbonyl group of D-glyceraldehyde established, while the 2"OH-group of D-glyceraldehyde showed hydrogen bonding with the amide oxygen of NADPH, His110, and Trp48 [45]. Visualize the 2D binding pose of compound 5 and tolrestat against the aldose reductase enzyme (PDB ID 1Z89) proposed in **Figure 5**.

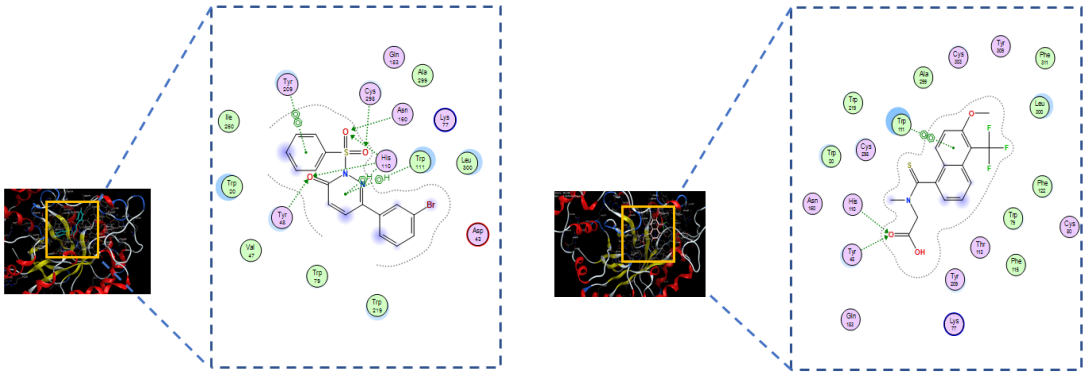

(a) (b)

Figure 5 Binding poses of (a) compound 5 and (b) tolrestat on the active site of aldose reductase enzyme (PDB ID 1Z89).

Even though compounds 6a - 6d have higher bond-free energy (S) values than the tolrestat positive control, they just form 2 hydrogen bonds with His 110 and Tyr48 and 2 hydrophobic interactions, namely π-π stacking contact with Trp111 and π-H stacking contact with Trp20.

Based on observations, the structure of the tested ligands lies within the active site, where the carbonyl group of the pyridazinone ring of compound **5**, the carbonyl group of the aliphatic ester from 6a - 6d, and the native sulfonyl-pyridazinone face towards the anion portion of the polar-binding pocket which is enclosed by H-bond donors and several aromatic rings from the catalytic residues Tyr 48, His 110, Trp111, Trp20 and Lys77 [43]. The pyridazinone ring portion of compound 5, 6a - 6d and the native ligand extend in the middle of the high hydrophobic site or selectivity pocket, while the aromatic ring portion is at the end site which consists of residues Thr113, Phe122, Leu300, and Cys303 [47].

Therefore, it is predicted that the tested ligands have antagonistic activity or being aldose reductase inhibitors, particularly the excellent value of binding free energy, the high percentage of residue contact, and the similarity of the interaction of the test ligand with critical residues.

ADME Properties

Here, ADME analysis was carried out on compounds 5 and 6a - 6d, because based on molecular docking studies previously, these compounds have potential as aldose reductase inhibitor agents. Therefore, an analysis of pharmacokinetic properties and safety for a drug candidate must be carried out before the drug is used on the target. High throughputs pharmacokinetic, such as adsorption, distribution, metabolism, excretion, and toxicity (ADMET) profiles using *in silico* model research is an *in vitro* screening to anticipate failures of drugs caused by undesirable properties of pharmacokinetic compounds in drug candidate development [47].

The bioavailability profiles showed that all synthesized compounds comply with Lipinski's rule of 5 (**Table 2**).

Table 2 Lipinski's rule of 5 properties of pyridazinone derivatives.

Lipinski's rule of 5 properties	Compounds				
	5	**6a**	**6b**	**6c**	**6d**
Molecular weight	391	288	288	288	337
Hydrogen bond donor	0	0	0	0	0
Hydrogen bond acceptor	4	5	5	5	4
LogP	3.99	1.48	1.48	1.48	2.24

Drug candidates (Compound 5 and 6a - 6d) that comply with Lipinski's 5 rules are said to have druglikeness properties [48,49] because they have good bioavailability properties and can be absorbed by moving across the gastrointestinal membrane into the bloodstream [50]. The solubility and permeability of drugs through membranes that are given orally are related to molecular size, lipophilicity, hydrogen bonds, and partition coefficients [31].

The bioavailability profile of pyridazinone derivatives shows that all synthesized compounds have complied with Lipinski's 5 rules (**Table 2**). The molecular weights of all selected ligands fall within the range of 288 - 391, which is approximately 500. Drug molecules with appropriate molecular weights are expected to quickly diffuse through cell membranes, causing high pharmacological activity against biological targets. Additionally, the quantity of donors (0) and hydrogen bond acceptors (4 - 5) is suitable. This means that the compound has excellent binding affinity and selectivity to biological targets. The log *p*-values of all compounds were within the acceptable range of 1.48 - 3.99, indicating that they were predicted to be able to pass through lipid bilayer membranes due to their good lipophilicity.

The Pharmacokinetic prediction (ADME profiles) of the compounds performed using pre-ADME (**Table 3**). Blood Brain Barrier (BBB) penetration values of compound 5 showed a percentage of 2.37 which means that the compound has a high absorption capacity of the CNS. While compounds 6a - 6d in the range from 0.13 to 0.78, lead to moderate absorption into the Central Nervous System (CNS). The extent to which a drug can penetrate the blood-brain barrier can have an impact on the CNS. Aldose reductase is expressed in all target tissues that are complicated by diabetes. In the brain, aldose reductase is found in various cells, primarily the Schwann cells of peripheral nerves, including neurons and glial cells, which play a significant role in diabetic peripheral neuropathy (DPN). In hyperglycemic conditions, the polyol pathway's hyperactivity in the peripheral nervous system (PNS) leads to neuropathies. Epalrestat is one of the aldose reductase inhibitor agents that can treat diabetic neuropathy. Experimental studies indicate that epalrestat reduces sorbitol accumulation in the sciatic nerve, erythrocytes, and ocular tissues in animals, and in erythrocytes in humans [51]. Other research has also shown that sulfonylurea and biguanide-based diabetes medicines can quickly cross the blood-brain barrier and start a number of molecular signaling pathways that improve memory and cognitive function in both mice and people [52]. Banks [53] found that statins or N-acetylcysteine can reverse the BBB opening in some models of DM. In addition, N-acetylcysteine, combined with insulin, alleviates the oxidative damage to the cerebrum by regulating redox homeostasis in type 1 diabetic mellitus canines, where NAC can cross the cell membrane and the blood-brain barrier and rapidly accumulate in peripheral organs [54]. Based on the above studies, the high BBB properties of the target compound are expected to also provide a positive effect for the therapy of diabetes complications. However, further research is needed to determine the potential implications of the CNS effects in the context of diabetes complications on this target compound.

Compound 5 showed the highest binding to plasma proteins with a value of 97.08 % of PPB compared to others. Furthermore, the others are moderately bound to plasma proteins, ranging from 74.34 to 84.89 %, which means that the tested compound is predicted to have the ability to induce pharmacological action on the target protein. Plasma Protein Binding (PPB) indicates the free drug fraction available for distribution to various tissues. Drugs not tightly bound (free-form drugs) to plasma proteins easily bounded to their receptors (targets) or other tissues to cause a pharmacological response [55]. The length of time the drug binds to plasma proteins could affect the duration of pharmacology of drug administration.

HIA and Caco-2 models measured intestinal permeability and metabolism. The compounds 5 and 6a - 6d had a well-absorbed HIA profile with % HIA values ranging from 97.97 to 98.4 %. The Caco-2 cell permeability of compounds was middle permeability, ranging from 5.39 to 30.09 nm/s, indicating that pyridazinone derivatives can be absorbed by the human intestine. Caco-2 cell, a human colon epithelial cancer cell line, mimics the human intestinal epithelium, so that used as an evaluation model of intestinal permeability and the toxicity for the selection of drug discovery [56]. The acceptable percentage of HIA values and Caco-2 cell permeability of compounds 6a - 6d align with their drug-likeness properties above, suggesting their efficient oral absorption. When compared with other aldose reductase inhibitors (here are tolrestat and epalrestat), the target compound is predicted to have fairly safe ADMET properties that are almost the same as other inhibitors. The target compound is predicted to have fairly safe ADMET properties that are almost the same as other inhibitors (in this case tolrestat and epalrestat). However, when compared to tolrestat, compound 5 is predicted to have a better level of safety. According to the prediction results, tolrestat has hepatotoxic and immunotoxic properties. Based on the half-life of the compound (T1/2), compound 5 also has a faster half-life than tolrestat, so the hepatotoxicity of compound 5 is likely to be more minimal. Many aldose reductase inhibitors have been withdrawn from the market. In this regard, Tolrestat was withdrawn because of serious effects and reduced efficacy in subsequent clinical trials. Previous studies have shown that tolrestat can cause hepatocellular damage [57,58]. Only epalrestat, a carboxylic acid derivative ARI, is available on the market to date.

The toxicity results also shown in **Table 3** indicate that all the pyridazinone derivatives studied were nontoxicity. However, it should be noted that compound 5 was hepatotoxic. Some parts of compound 5 are active

and can be modified, namely the benzene part bound to the pyridazinone ring containing the electron-withdrawing group m-Br and the benzene part bound to sulfonyl. Modifying the variation of the electron-withdrawing or electron-pushing group or removing the group in the benzene part is predicted to be able to eliminate the hepatotoxic properties of the compound, thereby increasing its safety level. However, this modification must also consider its impact on the strength of the inhibitor activity of the target compound. Subsequently, rat acute oral toxicity test (LD_{50}) and classification of toxicity were determined based on the Globally Harmonized System (GSH). From **Table 3**, it can be seen that based on LD50 value, compounds 5 (1,250 mg/kg), 6a (1,600 mg/kg), and 6c (1,650 mg/kg) were classified in class 4 indicated "harmful if swallowed" belongs to GSH. This means that they were to be slightly acute toxic. Then, both 6b and 6d (2,400 mg/kg) are indicated as "may be harmful if swallowed", according to GSH. It means that all compounds were low toxic compounds.

Table 3 ADMET profiles of pyridazinone derivatives using pre-ADME and Protox II.

ADMET Properties	Compounds						
	5	**6a**	**6b**	**6c**	**6d**	**Tolrestat**	**Epalrestat**
ADME							
Human Intestinal Absorbtion (HIA) (%)[a]	97.70 well	97.97 well	97.97 well	97.97 well	98.14 well	98.79 well	99.51 well
Caco-2 Cell Permeability (nm/sec)[b]	5.39 middle	30.09 middle	27.39 middle	9.03 middle	26.72 middle	33.81 middle	21.44 middle
Skin Permeability	−2.02	−3.46	−3.48	−3.48	−3.33	−2.32	−3.03
Blood Brain Barriers (BBB) Penetration[c]	2.37 high	0.46 middle	0.13 middle	0.78 middle	0.40 middle	1.73 high	0.17 middle
Plasma Protein Binding (PPB) (%)[d]	97.08 strong	74.34 weakly	82.68 weakly	78.77 weakly	85.47 weakly	93.58 strong	97.79 strong
CYP_2C19 inhibition	Yes	Non	Non	Non	Non	Non	Non
CYP_2C9 inhibition	Yes	Non	Non	Non	Non	Non	Non
CYP_3A4 inhibition	Non	Non	Yes	Yes	Non	Non	Non
CYP_3A4 substrate	Non	Non	Non	Non	Non	Yes	Yes
T1/2	0.89 short	0.75 short	0.76 short	0.8 short	0.80 short	1.14 intermediet	1.06 intermediet
Toxicity							
Mutagenicity	inactive	inactive	inactive	inactive	inactive	inactive	inactive
hepatoxicity	active	inactive	inactive	inactive	inactive	active	inactive
Immunotoxicity	inactive	inactive	inactive	inactive	inactive	active	inactive
Carcinogenicity	inactive	inactive	inactive	inactive	inactive	inactive	inactive
Rat acute oral toxicity (LD_{50}) (mg/kg)	1,260	1,600	2,400	1,650	2,400	2,250	5
Class[e]	4	4	5	4	5	5	2

[a]HIA: 0 ~ 20 % (poorly absorbed compounds); 20 ~ 70 % (moderately absorbed compounds); 70 ~ 100 (well absorbed compounds)

[b]Caco-2 cell permeability; < 4 (low permeability); 4 ~ 70 (middle permeability); > 70 (high permeability)

[c]BBB: > 2.0 (high absorbtion to CNS); 2.0 ~ 0.1 (middle absorbtion to CNS); < 0.1(low absorbtion to CNS)

[d]PPB: > 90 % (Strongly bound); < 90 % (weakly bound)

[e]Class: Class I: Fatal if swallowed (LD50 ≤ 5); Class II: Fatal if swallowed (5 < LD50 ≤ 50); Class III: Toxic if swallowed (50 < LD50 ≤ 300); Class IV: Harmful if swallowed (300 < LD50 ≤ 2,000); Class V: May be harmful if swallowed (2,000 < LD50 ≤ 5,000); Class VI: Non-toxic (LD50 > 5,000)

For future study, molecular dynamics methods are expected to strengthen the research results. However, in this study, the researchers focused solely on the docking phase. This is because, based on previous studies, it has been proven that bioactivity predictions through the molecular docking study approach with RMSD values < 2, the smaller the binding free energy value, and the conformation of ligand binding with important residues on the receptor, show results that are in line with the results *of in vitro* studies [59,60].

Conclusions

In this research, pyridazinone derivatives (4a - 4d, 5, and 6a - 6d) were successfully synthesized. The compound structures were confirmed by IR, H-NMR, and MS spectrophotometers. Generally, based on the docking results, it could be assumed that compounds 6a - 6d have middle inhibitory activity against aldose reductase (PDB ID 1Z89) using the molecular docking approach. That is the pyridazinone derivative compound 5 that is the best at blocking aldose reductase (PDB ID 1Z89). Based on Lipinski's Rule of 5 and ADMET profiles, pyridazinone derivatives (5 and 6a - 6d) exhibited safe properties as drug candidates. However, structural modification of compound 5 is required to eliminate the effect of hepatotoxicity. Further research, such as molecular dynamic approaches, *in vitro*, and *in vivo* tests, are needed to determine the potential bioactivity of pyridazinone derivative compounds, especially compound 5, as aldose reductase enzyme inhibitors. Therefore, compound 5 can be considered as a reference for further drug design development to be a potential agent for aldose reductase enzyme inhibitors.

Acknowledgements

This article is especially dedicated to the memory of our dear colleague, Prof. Dr. Adel Zamri, MS, DEA. Thank you Department of Chemistry, Faculty of Mathematics and Natural Sciences, Universitas Riau, Indonesia for providing the research equipment and materials. The authors would like to thank the postgraduate of Riau University and Direktorat Riset & Pengabdian Masyarakat (DPRM) KEMENRISTEK DIKTI through Doctoral Dissertation grant with contract number 390/UN.19.5.1.3/PT.01.03/2020 for generous financial support in completing this work.

References

[1] R Kumar, P Saha, Y Kumar, S Sahana, A Dubey and P Om. A Review on diabetes mellitus: Type1 & type2. *World Journal of Pharmacy and Pharmaceutical Sciences* 2020; **9(10)**, 838-850.

[2] SA Antar, NA Ashour, M Sharaky, M Khattab, NA Ashour, RT Zaid, EJ Roh, A Elkamhawy and AA Al-Karmalawy. Diabetes mellitus: Classification, mediators, and complications; A gate to identify potential targets for the development of new effective treatments. *Biomedicine and Pharmacotherapy* 2023; **168**, 115734.

[3] IW Suryasa, M Rodriguez-Gamez and T Koldoris. Health and treatment of diabetes mellitus. *International Journal of Health Sciences* 2021; **5(1)**, 1-5.

[4] L Cloete. Diabetes mellitus: an overview of the types, symptoms, complications and management. *Nursing Standard* 2022; **37(1)**, 61-66.

[5] D Tomic, JE Shaw and DJ Magliano. The burden and risks of emerging complications of diabetes mellitus. *Nature Reviews Endocrinology* 2022; **18(9)**, 525-539.

[6] S Jannapureddy, M Sharma, G Yepuri, AM Shcmidt and R Ramasamy. Aldose reductase: An emerging target for development of interventions for diabetic cardiovascular complications. *Frontiers in Endocrinology* 2021; **12**, 636267.

[7] M Singh, A Kapoor and A Bhatnagar. Physiological and pathological roles of aldose reductase. *Metabolites* 2021; **11(10)**, 655.

[8] M Bekhit and W Gorski. Determination of sorbitol dehydrogenase in microsamples of human serum. *Talanta* 2021; **235**, 122730.

[9] S Thakur, SK Gupta, V Ali, P Singh and M Verma. Aldose reductase: A cause and a potential target for the treatment of diabetic complications. *Archives of Pharmacal Research* 2021; **44(7)**, 655-667.

[10] AS Grewal, S Bhardwaj, D Pandita, V Lather and BS Sekhon. Updates on aldose reductase inhibitors for management of diabetic complications and non-diabetic diseases. *Mini-Reviews in Medicinal Chemistry* 2016; **16(2)**, 120-162.

[11] C Iacobini, M Vitale, C Pesce, G Pugliese and S Menini. Diabetic complications and oxidative stress: A 20-year voyage back in time and back to the future. *Antioxidants* 2021; **10(5)**, 727.

[12] Q Jin and RCW Ma. Metabolomics in diabetes and diabetic complications: Insights from epidemiological studies. *Cells* 2021; **10(11)**, 2832.

[13] S Ahmad, MFA Ahmad, S Khan, S Alouffi, M Khan, C Prakash, MWA Khan and IA Ansari. Exploring aldose reductase inhibitors as promising therapeutic targets for diabetes-linked disabilities. *International Journal of Biological Macromolecules* 2024; **280**, 135761.

[14] A Danila, LA Ghenciu, ER Stoicescu, SL Bolintineanu, R Iacob, M Sandesc and AC Faur. Aldose reductase as a key target in the prevention and treatment of diabetic retinopathy: A comprehensive review. *Biomedicines* 2024; **12(4)**, 747.

[15] P Kumari, R Kohal, Bhavana, GD Gupta and SK Verma. Selectivity challenges for aldose reductase inhibitors: A review on comparative SAR and interaction studies. *Journal of Molecular Structure* 2024; **1318**, 139207.

[16] M Imran and Abida. 6-(4-aminophenyl)-4,5-dihydro-3(2H)-pyridazinone - an important chemical moiety for development of cardioactive agents: A review. *Tropical Journal of Pharmaceutical Research* 2016; **15(7)**, 1579-1590.

[17] MMF Ismail, DHS Soliman, MHA Elmoniem and GARA Jaleel. Synthesis, molecular modeling of novel substituted pyridazinones and their vasorelaxant activities. *Medicinal Chemistry* 2020; **17(2)**, 171-186.

[18] AF Selim, FA Yassin and AM Salama. Green synthesized pyridazinone derivatives as promising biologically active and anticancer drugs. *Egyptian Journal of Chemistry* 2022; **65(3)**, 435-445.

[19] MKS El-Nagar, MI Shahin, MF El-Behairy, ES Taher, MF El-Badawy, M Sharaky, DAAE Ella, KAM Abouzid and M Adel. Pyridazinone-based derivatives as anticancer agents endowed with anti-microbial activity: Molecular design, synthesis, and biological investigation. *RSC Medicinal Chemistry* 2024; **15(10)**, 3529-3557.

[20] S Daoui, S Direkel, MM Ibrahim, B Tuzun, T Chelfi, M Al-Ghorbani, M bouatia, ME Karbane, A Doukkali, N Benchat and K Karrouchi. Synthesis, spectroscopic characterization, antibacterial activity, and computational studies of novel pyridazinone derivatives. *Molecules* 2023; **28(2)**, 678.

[21] MM Almehmadi, AA Alsaiari and M Asif. Synthesis and *in-vitro* antimycobacterial evaluation of 4-Arylidene-2-Phenyl-6-(Aryl)-4,5-Dihydropyridazin-3(2H)-One derivatives. *Pharmaceutical Chemistry Journal* 2023; **57(2)**, 265-273.

[22] EM Ahmed, AE Kassab, AA El-Malah and MSA Hassan. Synthesis and biological evaluation of pyridazinone derivatives as selective COX-2 inhibitors and potential anti-inflammatory agents. *European Journal of Medicinal Chemistry* 2019; **171**, 25-37.

[23] EO Osman, NA Khalil, A Magdy and Y El-Dash. Pyridazine and pyridazinone derivatives: Synthesis and in vitro investigation of their anti-inflammatory potential in LPS-induced RAW264.7 macrophages. *Drug Development Research* 2024; **85(2)**, e22173.

[24] I Allart-Simon, A Moniot, N Bisi, M Ponce-Vargas, S Audonnet, M Laronze-Cochard, J Sapi, E Henon, F Velard and S Gerard. Pyridazinone derivatives as potential anti-inflammatory agents: synthesis and biological evaluation as PDE4 inhibitors. *RSC Medicinal Chemistry* 2021; **12(4)**, 584-592.

[25] A Kotynia, E Krzyzak, J Zadło, M Witczak, L Szczukowski, J Mucha, P Swiatek and A Marciniak. Anti-Inflammatory and antioxidant pyrrolo[3,4-d]pyridazinone derivatives interact with dna and bind to plasma proteins—spectroscopic and *in silico* studies. *International Journal of Molecular Sciences* 2024; **25(3)**, 1784.

[26] Z Ozdemir, MA Alagoz, AG Akdemir, AB Ozcelik, B Ozçelik and M Uysal. Studies on a novel series of 3(2H)-pyridazinones: Synthesis, molecular modelling, antimicrobial activity. *Journal of Research in Pharmacy* 2019; **23(5)**, 960-972.

[27] HA Allam, AA Kamel, M El-Daly and RF George. Synthesis and vasodilator activity of some

pyridazin-3(2H)-one based compounds. *Future Medicinal Chemistry* 2020; **12(1)**, 37-50.

[28] F Chaudhry, AQ Ather, MJ Akhtar, A Shaukat, M Ashraf, M Al-Rashida, MA Munawar and MA Khan. Green synthesis, inhibition studies of yeast α-glucosidase and molecular docking of pyrazolylpyridazine amines. *Bioorganic Chemistry* 2017; **71**, 170-180.

[29] M Krasavin, A Shetnev, S Baykov, S Kalinin, A Nocentini, V Sharoyko, G Poli, T Tuccinardi, M Korsakov, TB Tennikova and CT Supuran. Pyridazinone-substituted benzenesulfonamides display potent inhibition of membrane-bound human carbonic anhydrase IX and promising antiproliferative activity against cancer cell lines. *European Journal of Medicinal Chemistry* 2019; **168**, 301-314.

[30] MF Sahin, B Badiccoglu, M Gokce, E Kupeli and E Yesilada. Synthesis and analgesic and antiinflammatory activity of methyl 6-substituted-3(2H)-pyridazinone-2-ylacetate derivatives. *Archiv der Pharmazie* 2004; **337(8)**, 445-452.

[31] F Balestri, R Moschini, U Mura, M Cappiello and AD Corso. In search of differential inhibitors of aldose reductase. *Biomolecules* 2022; **12(4)**, 485.

[32] Y Demir, FS Tokalı, E Kalay, C Turkes, P Tokalı, ON Aslan, K Sendil and S Beydemir. Synthesis and characterization of novel acyl hydrazones derived from vanillin as potential aldose reductase inhibitors. *Molecular Diversity* 2023; **27**, 1713-1733.

[33] K Askarova, S Mammadova, V Farzaliyev, A Sujayev, N Sadeghian, P Taslimi, N Kilinc, M Akkus, AR Sahin, S Alwasel and I Gulcin. Novel regioselective sulfamidomethylation of phenols: Synthesis, characterization, biological effects, and molecular docking study. *Journal of the Indian Chemical Society* 2024; **101(10)**, 101318.

[34] GE Said, HM Metwally, E Abdel-Latif, MR Elnagar, HS Ibrahim and MA Ibrahim. Development of non-acidic 4-methylbenzenesulfonate-based aldose reductase inhibitors; Design, synthesis, biological evaluation and *in-silico* studies. *Bioorganic Chemistry* 2024; **151**, 107666.

[35] C Turkes, Y Demir, A Bicer, GT Cin, MS Gultekin and S Beydemir. Exploration of some bis-sulfide and bis-sulfone derivatives as non-classical aldose reductase inhibitors. *ChemistrySelect* 2023; **8(5)**, e202204350.

[36] Y Dundar, O Kuyrukcu, G Eren, FSS Deniz, T Onkol and IE Orhan. Novel pyridazinone derivatives as butyrylcholinesterase inhibitors. *Bioorganic Chemistry* 2019; **92**, 103304.

[37] S Cruz, D Cifuentes, N Hurtado and M Roman. Sintesis de piridazin-3(2H)-onas asistida por microondas en condiciones libre de disolvente. *Informacion Tecnologica* 2016; **27(5)**, 57-62.

[38] D Kweon, H Kim, J Kim, HA Chung, Y Yoon, WS Lee and S Kim. Arenesulfonylheterocycles (I): Synthesis and reactions of 2-benzenesulfonyl-4, 5-dichloropyridazin-3-ones with amines. *Journal of Heterocyclic Chemistry* 2002; **39(1)**, 203-211.

[39] H Steuber, M Zentgraf, A Podjarny, A Heine and G Klebe. High-resolution crystal structure of aldose reductase complexed with the novel sulfonyl-pyridazinone inhibitor exhibiting an alternative active site anchoring group. *Journal of Molecular Biology* 2006; **356(1)**, 45-56.

[40] D Obermayer, D Znidar, G Glotz, A Stadler, D Dallinger and CO Kappe. Design and performance validation of a conductively heated sealed-vessel reactor for organic synthesis. *Journal of Organic Chemistry* 2016; **81(23)**, 11788-11801.

[41] R Cachau, E Howard, P Barth, A Mitschler, B Chevrier, V Lamour, A Lamour, A Joachimiak, R Sanishvili, MV Zandt, E Sibley, D Moras and A Podjarny. Model of the catalytic mechanism of human aldose reductase based on quantum chemical calculations. *Journal de Physique IV* 2000; **10(10)**, Pr10-3 - Pr10-13.

[42] M Yaeghoobi, N Frimayanti, CF Chee, KK Ikram, BO Najjar, SM Zain, Z Abdullah, HA Wahab and NA Rahman. QSAR, *in silico* docking and *in vitro* evaluation of chalcone derivatives as potential inhibitors for H1N1 virus neuraminidase. *Medicinal Chemistry Research* 2016; **25(10)**, 2133-2142.

[43] A Urzhumtsev, F Tete-Favier, A Mitschler, J Barbanton, P Barth, L Urzhumtseva, J Biellmann, AD Podjarny and D Moras. A “specificity” pocket inferred from the crystal structures of the complexes of aldose reductase with the

pharmaceutically important inhibitors tolrestat and sorbinil. *Structure* 1997; **5(5)**, 601-612.

[44] M Meyer, P Wilson and D Schomburg. Hydrogen bonding and molecular surface shape complementarity as a basis for protein docking. *Journal of Molecular Biology* 1996; **264(1)**, 199-210.

[45] YS Lee, M Hodoscek, BR Brooks and PF Kador. Catalytic mechanism of aldose reductase studied by the combined potentials of quantum mechanics and molecular mechanics. *Biophysical Chemistry* 1998; **70(3)**, 203-216.

[46] MG Salem, YAA Aziz, M Elewa, MS Nafie, HA Elshihawy and MM Said. Synthesis, molecular modeling, selective aldose reductase inhibition and hypoglycemic activity of novel meglitinides. *Bioorganic Chemistry* 2021; **111**, 104909.

[47] A Kousaxidis, A Petrou, V Lavrentaki, M Fesatidou, I Nicolaou and A Geronikaki. Aldose reductase and protein tyrosine phosphatase 1B inhibitors as a promising therapeutic approach for diabetes mellitus. *European Journal of Medicinal Chemistry* 2020; **207**, 112742.

[48] M Rashid. Design, synthesis and ADMET prediction of bis-benzimidazole as anticancer agent. *Bioorganic Chemistry* 2020; **96**, 103576.

[49] S Tian, J Wang, Y Li, D Li, L Xu and T Hou. The application of *in silico* drug-likeness predictions in pharmaceutical research. *Advanced Drug Delivery Reviews* 2015; **86**, 2-10.

[50] CM Chagas, S Moss and L Alisaraie. Drug metabolites and their effects on the development of adverse reactions: Revisiting lipinski's rule of five. *International Journal of Pharmaceutics* 2018; **549(1-2)**, 133-149.

[51] MA Ramirez and NL Borja. Epalrestat: An aldose reductase inhibitor for the treatment of diabetic neuropathy. *Pharmacotherapy* 2008; **28(5)**, 646-655.

[52] H Yaribeygi, M Ashrafizadeh, NC Henney, T Sathyapalan, T Jamialahmadi and A Sahebkar. Neuromodulatory effects of anti-diabetes medications: A mechanistic review running. *Pharmacological Research* 2020; **152**, 104611.

[53] WA Banks. The blood-brain barrier interface in diabetes mellitus: Dysfunctions, mechanisms and approaches to treatment. *Current Pharmaceutical Design* 2020; **26(13)**, 1438-1447.

[54] X Li, H Wu, H Huo, F Ma, M Zhao, Q Han, L Hu, Y Li, H Zhang, J Pan, Z Tang and J Guo. N-acetylcysteine combined with insulin alleviates the oxidative damage of cerebrum via regulating redox homeostasis in type 1 diabetic mellitus canine. *Life Sciences* 2022; **308**, 120958.

[55] SK Singh, GR Valicherla, AK Bikkasani, SH Cheruvu, Z Hossain, I Taneja, H Ahmad, KSR Raju, NS Sangwan, SK Singh, AK Dwiedi, M Wahajuddin and JR gayen. Elucidation of plasma protein binding, blood partitioning, permeability, CYP phenotyping and CYP inhibition studies of Withanone using validated UPLC method: An active constituent of neuroprotective herb Ashwagandha. *Journal of Ethnopharmacology* 2021; **270**, 113819.

[56] J Qiu, J Zhang and A Li. Cytotoxicity and intestinal permeability of phycotoxins assessed by the human Caco-2 cell model. *Ecotoxicology and Environmental Safety* 2023; **249**, 114447.

[57] BL Bernardoni, I D'Agostino, F Sciano and CL Motta. The challenging inhibition of aldose reductase for the treatment of diabetic complications: A 2019-2023 update of the patent literature. *Expert Opinion on Therapeutic Patents* 2024; **34(11)**, 1085-1103.

[58] S Ryder, B Sarokhan, DG Shand and JF Mullane. Human safety profile of tolrestat: An aldose reductase inhibitor. *Drug Development Research* 1987; **11(2)**, 131-143.

[59] B Sever, MD Altıntop, Y Demir, N Yılmaz, GA Ciftci, S Beydemir and A Ozdemir. Identification of a new class of potent aldose reductase inhibitors: Design, microwave-assisted synthesis, *in vitro* and *in silico* evaluation of 2-pyrazolines. *Chemico-Biological Interactions* 2021; **345**, 109576.

[60] G Yapar, HE Duran, N Lolak, S Akocak, C Turkes, M Durgun, M Isik and S Beydemir. Biological effects of bis-hydrazone compounds bearing isovanillin moiety on the aldose reductase. *Bioorganic Chemistry* 2021; **117**, 105473.